Influence of Large-Scale Flow Regimes on Cool-Season Precipitation in the Northeastern United States

HEATHER M. ARCHAMBAULT, LANCE F. BOSART, DANIEL KEYSER, AND ANANTHA R. AIYYER*

University at Albany, State University of New York, Albany, New York

(Manuscript received 17 July 2007, in final form 28 November 2007)

ABSTRACT

The influence of large-scale flow regimes on cool-season (November–April) northeastern U.S. (Northeast) precipitation is investigated for the period 1948–2003 from statistical and synoptic perspectives. These perspectives are addressed through (i) a statistical analysis of cool-season Northeast precipitation associated with the North Atlantic Oscillation (NAO) and Pacific–North American (PNA) regimes (one standard deviation or greater NAO or PNA daily index anomalies persisting several days), and (ii) a composite analysis of the synoptic signatures of major (two standard deviation) 24-h cool-season Northeast precipitation events occurring during NAO and PNA regimes. The statistical analysis reveals that negative PNA regimes are associated with above-average cool-season Northeast precipitation and an above-average frequency of light and moderate precipitation events, whereas the opposite associations are true for positive PNA regimes. In comparison with PNA regimes, NAO regimes are found to have relatively little influence on the amount and frequency of cool-season Northeast precipitation. The composite analysis indicates that a surface cyclone flanked by an upstream trough over the Ohio Valley and downstream ridge over eastern Canada and upper- and lower-level jets in the vicinity of the Northeast are characteristic signatures of major cool-season Northeast precipitation events occurring during NAO and PNA regimes. Negative NAO and positive PNA precipitation events, however, are associated with a more amplified trough–ridge pattern and greater implied Atlantic moisture transport by a low-level jet into the Northeast than positive NAO and negative PNA precipitation events. Furthermore, a signature of lateral upper-level jet coupling is noted only during positive and negative PNA precipitation events.

1. Introduction

The tendency for certain extratropical large-scale flow regimes to recur is documented extensively in the literature. Such regimes include high- and low-index flows (Rossby 1939; Rossby and Willett 1948; Namias 1950), blocking (Rex 1950a,b; Pelly and Hoskins 2003), persistent circulation anomalies (Dole and Gordon 1983; Dole 1986; Branstator 1995), teleconnection patterns, such as the North Atlantic Oscillation (NAO; Walker and Bliss 1932; Wallace and Gutzler 1981; Barnston and Livezey 1987; Feldstein 2003) and the Pacific–North American (PNA) pattern (Wallace and Gutzler 1981; Barnston and Livezey 1987; Feldstein 2002), and annular modes of low-frequency variability such as the Arctic Oscillation (AO; Thompson and Wallace 1998, 2000)/Northern Hemisphere (NH) Annular Mode (NAM; Wallace 2000). Following landmark studies on extratropical NH teleconnections by Wallace and Gutzler (1981) and Barnston and Livezey (1987), recent research has shown that the NAO/AO/NAM and the PNA pattern explain a significant amount of the low-frequency variance of geopotential height (or height), streamfunction, and sea level pressure (SLP) fields in the extratropical NH (Quadrelli and Wallace 2004) and exert a powerful influence on regional climates (e.g., Leathers et al. 1991; Hurrell 1995; Notaro et al. 2006).

The NAO consists of a north–south-oriented dipole of opposing SLP or midlevel height anomalies over the

* Current affiliation: Department of Marine, Earth, and Atmospheric Sciences, North Carolina State University, Raleigh, North Carolina.

Corresponding author address: Heather M. Archambault, Dept. of Earth and Atmospheric Sciences, University at Albany, State University of New York, ES-234, 1400 Washington Ave., Albany, NY 12222.
E-mail: heathera@atmos.albany.edu

DOI: 10.1175/2007MWR2308.1

North Atlantic Ocean and manifests as an alternation between an anomalously strong and anomalously weak North Atlantic jet stream (the positive and negative phases of the NAO). The related AO/NAM is an annular mode of NH low-frequency variability that includes a third anomaly center over the North Pacific Ocean in addition to the North Atlantic NAO anomaly dipole. In addition to influencing the strength and location of the jet stream over the North Atlantic and North Pacific, the AO/NAM impacts the atmospheric mass distribution in the NH extratropics and polar region. Despite conceptual differences between the NAO and AO/NAM, time series of daily indices measuring their strengths are highly correlated (Deser 2000; Ambaum et al. 2001; Feldstein and Franzke 2006) because of the overlap of their domains and some similarity in their definition.

The PNA pattern, another important teleconnection pattern in the extratropical NH, is a stationary Rossby wave train–like pattern that originates in the tropical central Pacific and arcs along a great circle to the southeastern United States. During the positive PNA phase, midlevel height anomalies are positive near Hawaii and the intermountain region of North America and negative in the vicinity of the Aleutian Islands and the southeastern United States, corresponding to an anomalously strong jet stream over the eastern Pacific. During the negative PNA phase, the signs of midlevel height anomalies over the Pacific and North America are opposite those associated with the positive PNA phase and correspond to an anomalously weak jet stream over the eastern Pacific.

Recurrent large-scale flow regimes impact precipitation amount and frequency in some extratropical NH regions because they influence storm tracks and modulate the location and strength of moisture transport and convergence. During the positive NAO phase, the mean North Atlantic storm track parallels the eastern North American coastline before extending northeastward to near Iceland (Rogers 1990). This storm track and its associated moisture transport and convergence favor relatively wet conditions near the eastern U.S. coast and northern Europe, and relatively dry conditions across central and southern Europe (Hurrell 1995). During the negative NAO phase, on the other hand, the mean North Atlantic storm track is more zonal (Rogers 1990), favoring relatively wet conditions across central and southern Europe, and relatively dry conditions near the eastern U.S. coast and northern Europe (Hurrell 1995). During the positive PNA phase, the mean storm track over eastern North America is farther equatorward than usual, enhancing precipitation over the Gulf Coast and southeastern United States and suppressing precipitation over the upper Mississippi and Ohio Valleys. Conversely, during the negative PNA phase, the mean storm track over eastern North America is farther poleward than usual, enhancing precipitation over the upper Mississippi and Ohio Valleys and suppressing precipitation over the Gulf Coast and southeastern United States (Leathers et al. 1991; Notaro et al. 2006).

Building upon prior research linking recurrent large-scale flow regimes to regional precipitation patterns in the extratropical NH, the present study examines the influence of large-scale flow regimes on cool-season precipitation in the northeastern United States (Northeast) from 1948 through 2003. This study consists of (i) a statistical analysis of cool-season Northeast precipitation during NAO and PNA regimes, and (ii) a composite analysis of synoptic signatures of the onset of major 24-h cool-season Northeast precipitation events occurring during NAO and PNA regimes. Because dynamical models are able to skillfully predict the daily phase and amplitude of the NAO and PNA pattern as much as 2 weeks in advance during the cool season (Johansson 2007), it is anticipated that the results of this study will benefit forecasters making both short- and medium-range cool-season precipitation forecasts for the Northeast.

The methodology and datasets used in this study are described in section 2. A statistical analysis of cool-season Northeast precipitation anomalies during NAO and PNA regimes is documented in section 3. A composite analysis of synoptic-scale features at the onset of major cool-season Northeast precipitation events during NAO and PNA regimes is presented in section 4. The discussion and summary of the key findings follow in sections 5 and 6, respectively.

2. Data and methodology

a. Identification of NAO and PNA regimes

To identify NAO and PNA regimes objectively, daily NAO and PNA index times series are constructed for a 56-yr time period (1 January 1948–31 December 2003) from the 2.5° × 2.5° gridded 0000 and 1200 UTC National Centers for Environmental Prediction–National Center for Atmospheric Research (NCEP–NCAR) reanalysis (Kalnay et al. 1996; Kistler et al. 2001) 500-hPa geopotential height fields. The domains used to compute daily NAO and PNA index time series are the same as those used by the National Oceanic and Atmospheric Administration (NOAA)/Earth System Research Laboratory (ESRL)/Physical Sciences Division (PSD). Figure 1 shows the two NAO domains—the north (N; 55°–70°N, 70°–10°W) and south (S; 35°–45°N,

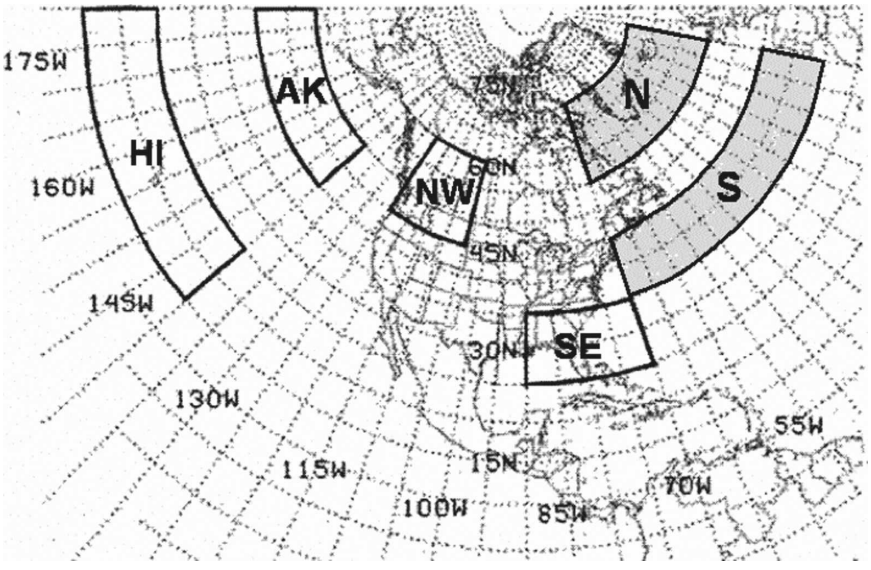

FIG. 1. The domains of the NAO (N and S domains; shaded) and the PNA pattern (HI, AK, NW, and SE domains; not shaded) used to create the daily index time series.

70°–10°W) domains—and the four PNA domains—the Hawaii (HI; 15°–25°N, 180°–140°W), Alaska (AK; 40°–50°N, 180°–140°W), Pacific Northwest (NW; 45°–60°N, 125°–105°W), and southeastern U.S. (SE; 25°–35°N, 90°–70°W) domains.

Time series of daily area-weighted domain-averaged 500-hPa geopotential height are calculated for each of the two NAO and four PNA domains. The values of the domain-averaged 500-hPa geopotential height for each day in the time series are standardized [e.g., Wilks 2006, Eq. (3.21), p. 47] by subtracting the 15-day-running long-term (i.e., 1948–2003) mean and then dividing by the corresponding 15-day-running long-term standard deviation. The standardized S domain time series is subtracted from the standardized N domain time series to create the standardized NAO index time series. To create the standardized PNA index time series, the standardized AK domain time series is subtracted from the standardized HI domain time series, and the standardized SE domain time series is subtracted from the standardized NW domain time series. The HI − AK time series is then added to the NW − SE time series. The NAO and PNA index time series are subsequently normalized by the standard deviations of the entire respective time series. This additional normalization ensures that the NAO and PNA index time series both have unit standard deviation (Wilks 2006, p. 49), thereby facilitating the objective identification of regimes in the respective time series.

Although there is no universally accepted method for constructing daily NAO and PNA index time series, the NOAA/ESRL/PSD and the NCEP/Climate Prediction Center (CPC) both provide daily NAO and PNA index time series that are used operationally on a widespread basis. As in the present study, the ESRL/PSD and the CPC use 500-hPa geopotential height data obtained from the NCEP–NCAR reanalysis to construct their time series. At the ESRL/PSD, the NAO and PNA index time series are constructed by calculating differences between standardized daily 500-hPa geopotential heights for fixed domains that correspond to the centers of action of the NAO and PNA patterns. These centers of action are identified using rotated principal component analysis (RPCA; Barnston and Livezey 1987). At the CPC, the NAO and PNA index time series are constructed by performing a least squares regression of the daily geopotential height field onto 10 seasonally varying teleconnection patterns, also identified using RPCA. The ESRL/PSD fixed domain method is chosen as the basis for the NAO and PNA index time series method used in this study because of its relative simplicity. Correlations between the teleconnection index time series generated for this study and at the ESRL/PSD are likely to be strong, but are not determined because of the lack of publicly available long-term ESRL/PSD time series. Despite major differences in methodology, strong correlations are found between the teleconnection time series generated in the present study and at the CPC: the NAO and the PNA time series correlation coefficients are 0.84 and 0.81, respectively, for the period 1 January 1950–31 December 2003.

Eight large-scale flow regimes, consisting of four individual and four combination regimes, are defined ob-

TABLE 1. The number of cool-season days that fall within each regime category.

Individual regime	Tot No. of days	Combination regime	Tot No. of days
+NAO	967	+NAO and +PNA	215
−NAO	1238	+NAO and −PNA	320
+PNA	1112	−NAO and +PNA	295
−PNA	1243	−NAO and −PNA	228

jectively using daily NAO and PNA indices. Table 1 shows the number of cool-season days that fall within each regime category. One of four individual regimes (positive NAO, negative NAO, positive PNA, and negative PNA) is considered to occur when a daily standardized NAO or PNA index value of ±1.0 (a one standard deviation anomaly) or greater persists for at least seven consecutive days. One of four combination regimes (positive NAO–positive PNA, positive NAO–negative PNA, negative NAO–positive PNA, and negative NAO–negative PNA) is considered to occur when a daily standardized NAO and PNA index value of ±1.0 persists for at least 3 days. A more relaxed persistence requirement is necessary for the identification of combination regimes to ensure an adequate sample size for statistical analysis.

b. Creation of a Northeast precipitation database

All precipitation data used in this research are obtained from the NCEP Unified Precipitation Dataset (UPD; Higgins et al. 2000). This dataset contains 24-h (1200–1200 UTC) precipitation amounts over a 56-yr period (1 January 1948–31 December 2003) for the region bounded by 20°–60°N, 140°–60°W. The UPD is gridded on a 0.25° × 0.25° mesh, and integrates NOAA first-order station precipitation measurements, daily cooperative observation measurements, and National Weather Service (NWS) River Forecast Center data.

A time series of daily Northeast precipitation anomalies is created as follows. (i) The average 24-h precipitation amount for the area bounded by the Canadian–U.S. border, the west Atlantic coast, 80°W, and 38°N (Fig. 2) is computed for each 1200–1200 UTC period between 1 January 1948 and 31 December 2003. (ii) Because the distribution of these precipitation data exhibits a strong positive skew (not shown), a power transformation is applied to make the precipitation distribution symmetric [Wilks 2006, Eq. (3.18a), p. 43]. Application of this transformation consists of raising each domain-averaged 24-h precipitation amount in the time series to a power λ; a value of λ equal to 0.19 is found to generate a nearly symmetric distribution. (iii)

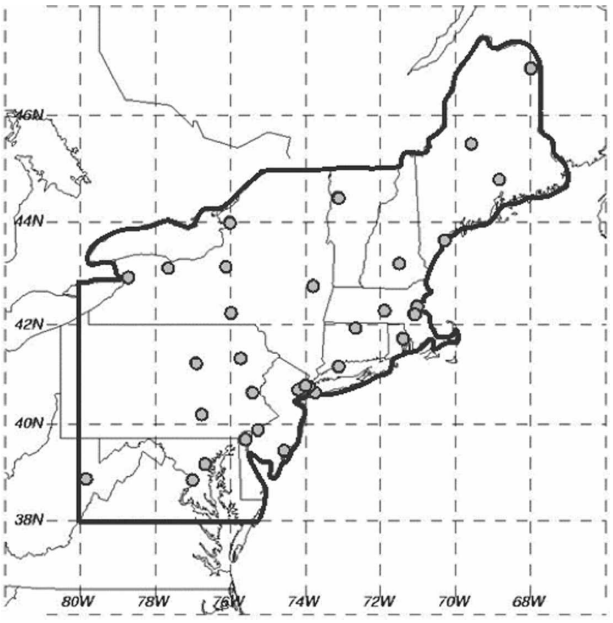

FIG. 2. The domain used to calculate the daily time series of Northeast precipitation anomalies. Gray circles indicate locations of the 32 first-order stations within the domain.

A standardized Northeast precipitation anomaly is computed for each 24-h period in the dataset by subtracting the running 7-day long-term mean of the transformed precipitation amount and dividing by the corresponding 7-day standard deviation. A statistical assessment of daily Northeast precipitation anomalies as a function of the spatial extent of the Northeast domain (not shown) suggests that the precipitation anomaly time series used in this study is relatively stable with respect to the spatial extent of the Northeast domain.

In this study, a 24-h Northeast precipitation event is categorized as major if the event is associated with a standardized 24-h Northeast precipitation anomaly of at least +2.0. A major Northeast precipitation event is considered a significant snow event if at least a 25-cm snowfall was recorded on the onset date of the event at one or more of the 32 first-order stations within the domain defined in Fig. 2. The daily snowfall data are obtained from the NOAA/National Environmental Satellite, Data, and Information Service/National Climatic Data Center Climatological Data monthly publications (information available online at http://www7.ncdc.noaa.gov/IPS/index.jsp).

c. Construction of composite analyses

To show the synoptic signatures of the onset of major cool-season Northeast precipitation events occurring during various large-scale flow regimes, combinations

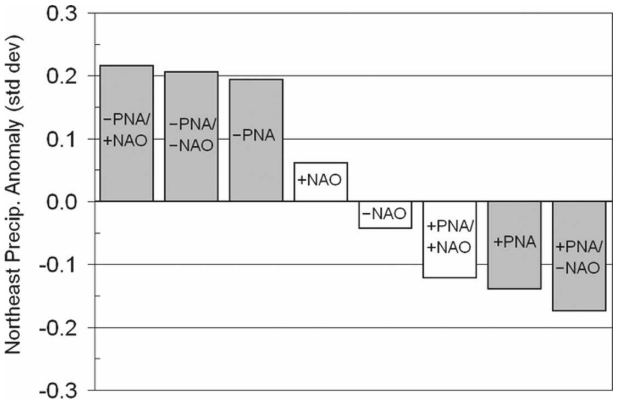

FIG. 3. Cool-season Northeast precipitation anomalies for eight large-scale flow regimes relative to the cool-season climatology. Shaded bars indicate statistical significance at the 99% confidence level as determined by a two-sided Student's *t* test.

of composite variables are calculated from the NCEP–NCAR reanalysis. Composite fields of 300-, 500-, and 850-hPa geopotential height, 300- and 850-hPa wind speed, 1000–500-hPa thickness, 700-hPa absolute vorticity, and SLP are calculated from data valid at the onset time (i.e., 1200 UTC) of the major precipitation events. In contrast, composite fields of 500-hPa geopotential height departures with respect to climatology [i.e., a 15-day-running long-term (i.e., 1948–2003) mean], 500-hPa vertical motion, and column-integrated precipitable water (PW) are calculated from daily averaged NCEP–NCAR reanalysis data valid for the onset dates of the major precipitation events. Daily averaged data are used to calculate composite fields of 500-hPa geopotential height departures from climatology and PW because of the lack of availability of higher-temporal-resolution data, and to calculate composite fields of 500-hPa vertical motion to obtain relatively smooth plots of vertical motion. Statistical significance of 500-hPa geopotential height departures from climatology is evaluated using a two-sided Student's *t* test (see, e.g., Wilks 2006, section 5.2.1, p. 139), which gives the probability that the composite 500-hPa geopotential height differs significantly from climatology.

A subjective comparison of 500-hPa geopotential height and SLP for all composite precipitation events with the individual cases constituting the composites finds that each composite case represents the individual cases in the composite reasonably well. It should be noted, however, that although compositing individual cases allows characteristic features of certain types of precipitation events to be identified, the smearing of features implicit in the compositing procedure indicates that mean intensities of features such as surface cyclones and upper-level jet streaks cannot be as reliably inferred (e.g., Lackmann et al. 1996; Sisson and Gyakum 2004).

TABLE 2. Northeast precipitation anomalies (std dev) associated with individual large-scale flow regimes by cool-season month.

	Northeast precipitation anomaly (std dev)			
Month	+NAO	−NAO	+PNA	−PNA
November	0.08	0.19	0.04	0.10
December	−0.04	0.03	−0.10	0.17
January	0.03	−0.01	−0.17	0.14
February	0.09	−0.12	−0.35	0.21
March	0.15	−0.16	−0.20	0.27
April	0.04	−0.18	0.14	0.31

3. Statistical analysis

The influence of various large-scale flow regimes on cool-season Northeast precipitation is assessed by calculating a composite cool-season Northeast precipitation anomaly associated with each of the four individual regimes and four combination regimes. The composite precipitation anomaly of each regime is obtained by averaging the precipitation anomalies of all cool-season days falling within each regime category (see Table 1 for the number of days in each regime category). The precipitation anomalies, shown in Fig. 3, reveal that cool-season Northeast precipitation tends to be above average during negative PNA regimes, and is most above average during the combination positive NAO–negative PNA regimes. Conversely, cool-season Northeast precipitation tends to be below average during cool-season positive PNA regimes, and is most below average during the combination negative NAO–positive PNA regimes. In contrast to PNA regimes, positive and negative NAO regimes are found to be associated with close-to-average cool-season precipitation.

To explore how Northeast precipitation–large-scale regime relationships vary throughout the cool season, precipitation anomalies associated with the four individual large-scale regimes are calculated for each cool-season month and displayed in Table 2. Results indicate that relationships between large-scale regimes and Northeast precipitation presented in Fig. 3 are relatively consistent throughout the cool season. It is found that negative PNA regimes are associated with above-average Northeast precipitation during all cool-season months, with the strongest associations found for February–April. Positive PNA regimes are associated with below-average precipitation for December–March, with the strongest associations found for February and

March. For the NAO regimes, precipitation is generally close to average throughout the cool-season months, with an exception noted for February–April, when Northeast precipitation tends to be below average during negative NAO regimes.

To obtain information about the frequency of Northeast precipitation events of varying magnitudes as a function of large-scale flow regime, the frequency distributions of 24-h cool-season Northeast precipitation anomalies associated with the four individual regimes, as well as frequency differences from cool-season climatology, are constructed and presented in Fig. 4. Consistent with Fig. 3 and Table 2, Fig. 4 indicates that precipitation anomaly distributions differ more significantly from climatology during cool-season PNA regimes (Figs. 4e–h) than during cool-season NAO regimes (Figs. 4a–d). During negative PNA regimes (Figs. 4g,h), light and moderate precipitation periods are more likely, whereas during positive PNA regimes (Figs. 4e,f), light and moderate precipitation periods are less likely. The precipitation distributions during cool-season NAO regimes generally are close to the cool-season climatological distribution (Figs. 4a–d), although major (2 standard deviations or greater) cool-season Northeast precipitation events appear to be slightly more likely during positive NAO regimes and slightly less likely during negative NAO regimes.

The percentage of days in the 56-yr dataset meeting the major cool-season Northeast precipitation event criteria during each of the individual large-scale regimes is computed and compared to the overall cool-season frequency in order to quantify the frequency of major cool-season Northeast precipitation events during the regimes. During positive NAO regimes, 3.1% of all cool-season days are associated with major Northeast precipitation events, a frequency that is slightly greater than the climatological frequency of 2.4% of cool-season days. During positive and negative PNA regimes, major cool-season Northeast precipitation events occur on 2.3% and 2.2% of cool-season days, respectively, whereas during negative NAO regimes, major precipitation events occur on 1.7% of cool-season days. Doubt is cast on the robustness of the slight departures from the climatological frequency of major cool-season Northeast precipitation events associated with NAO regimes, however, by results presented in Fig. 3 and Table 2, indicating that statistical relationships between cool-season Northeast precipitation and NAO regimes are weak.

To provide a complementary perspective on relationships between extreme cool-season Northeast precipitation and the large-scale flow pattern, standardized daily NAO and PNA indices are plotted as a function of the 24-h Northeast precipitation anomalies for the top-50 24-h cool-season Northeast precipitation events (ranked by precipitation anomaly relative to climatology) between 1948 and 2003 (displayed in Fig. 5). Inspection of Fig. 5a suggests a tendency for the NAO to be in a positive phase during extreme cool-season Northeast precipitation events, with a positive NAO phase observed for 39 of 50 events (78%). Of the top events, eight are found to occur during positive NAO regimes, and four during negative NAO regimes. The average daily NAO index during the top-50 precipitation events is +0.53, a value that is statistically significant at the 99% confidence level as determined by a two-sided Student's t test. A weaker tendency for the PNA pattern to be in a positive phase during extreme cool-season Northeast precipitation events is suggested by Fig. 5b, with a positive PNA phase observed for 30 of 50 events (60%). Of the top events, five are found to occur during positive PNA regimes, but six are found to occur during negative PNA regimes. The average PNA index during the top-50 precipitation events is +0.23, a value that is statistically significant at only the 85% confidence level as determined by a two-sided Student's t test.

The statistical results suggesting a tendency for both the NAO and the PNA pattern to be in a positive phase during extreme cool-season Northeast precipitation events are supported by a composite analysis of the onset of the top-50 24-h cool-season Northeast precipitation events (not shown). Consistent with the well-known characteristics of the positive phases of the NAO and the PNA pattern, the composite analysis displays an anomalously strong North Atlantic jet stream, and an amplified upper-level ridge and trough over the western and eastern United States, respectively.

4. Composite analysis

In section 3, PNA regimes were shown to influence the amount of cool-season precipitation received in the Northeast (Fig. 3, Table 2), as well as the frequency of Northeast precipitation events of varying magnitudes (Fig. 4). The present section explores the influence of NAO and PNA regimes on the synoptic-scale features of major (two standard deviation) 24-h cool-season Northeast precipitation events.

Composite analyses of the onset of all 30 major 24-h cool-season Northeast precipitation events occurring during positive NAO regimes (Table 3) are displayed in Fig. 6. These major precipitation events make up the extreme right tail of the positive NAO relative frequency distribution plot of 24-h precipitation anomalies (see Figs. 4a,b). In addition to occurring during positive

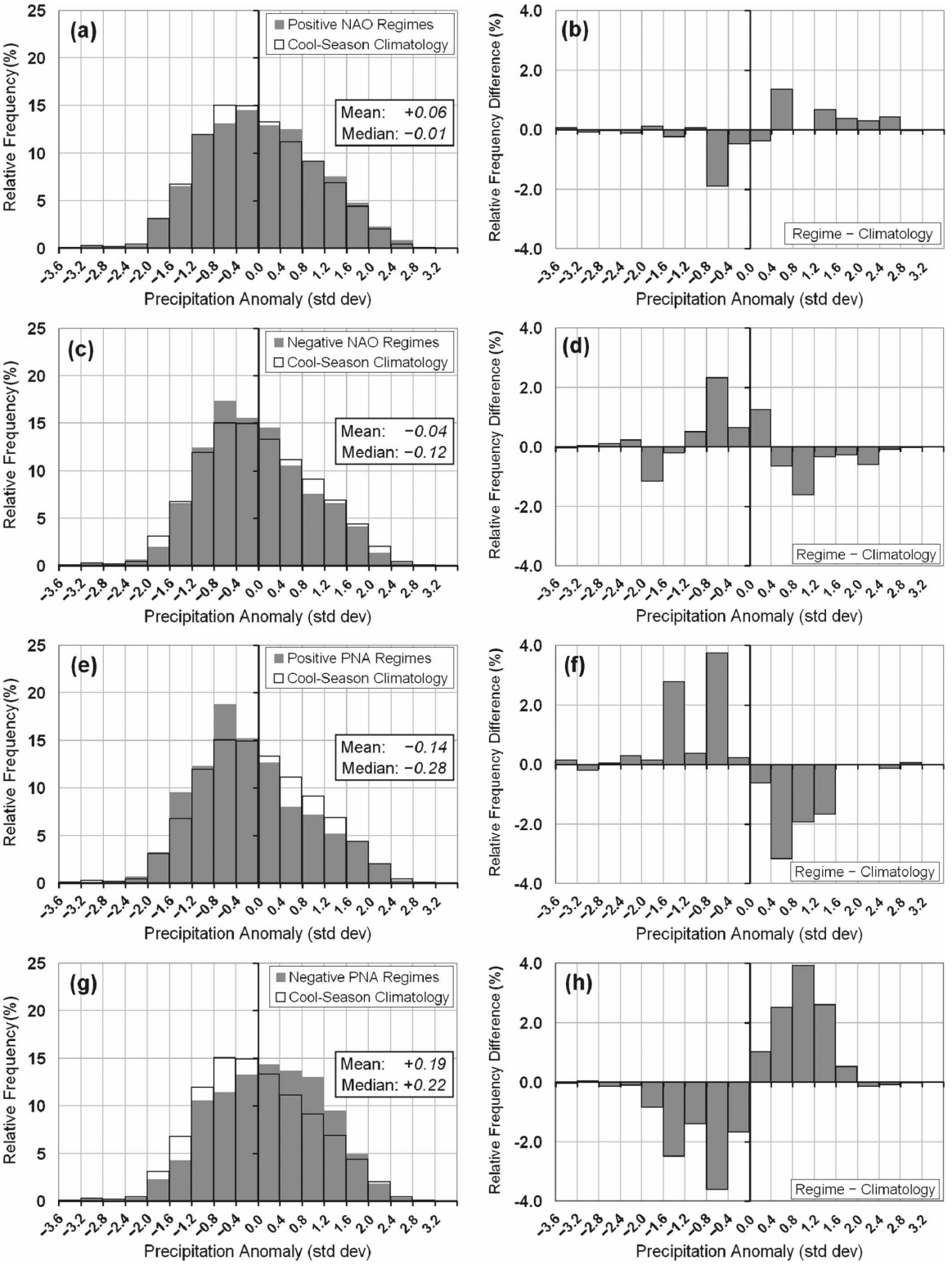

FIG. 4. The relative frequency (%) of 24-h cool-season Northeast precipitation anomalies during (a) positive NAO, (c) negative NAO, (e) positive PNA, and (g) negative PNA regimes (shaded); and the relative frequency difference from cool-season climatology (%) during (b) positive NAO, (d) negative NAO, (f) positive PNA, and (h) negative PNA regimes. The cool-season climatological relative frequency (%) of 24-h Northeast precipitation anomalies (not shaded) is included in (a), (c), (e), and (g) for comparison with the relative frequency of cool-season Northeast precipitation anomalies during large-scale flow regimes.

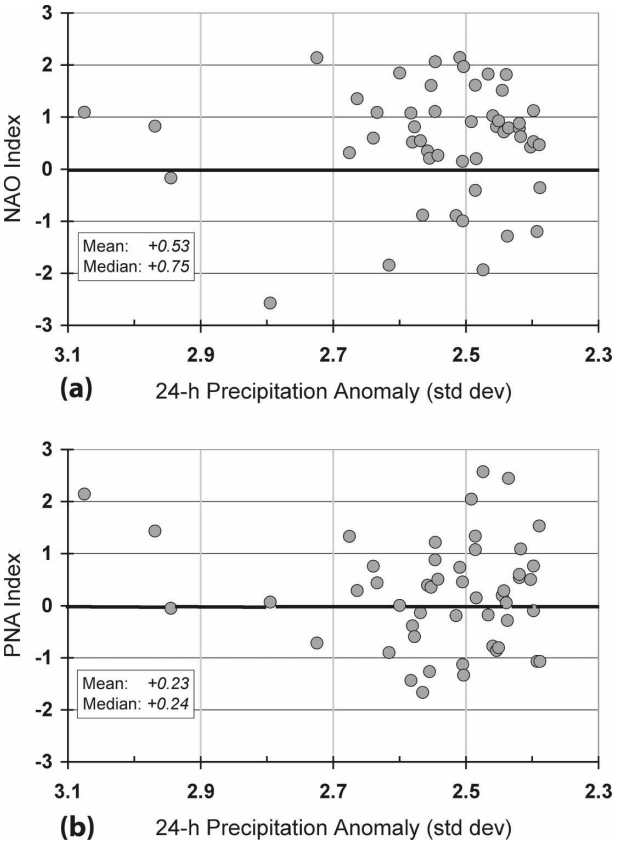

FIG. 5. Standardized daily (a) NAO and (b) PNA indices for the top-50 24-h cool-season Northeast precipitation events (1948–2003). Values of Northeast precipitation anomalies (std dev) on the abscissa increase from right to left.

TABLE 3. The 30 major 24-h (1200–1200 UTC) cool-season Northeast precipitation events occurring during positive NAO regimes (1948–2003). Events are listed in descending order of Northeast precipitation anomaly. Dates in boldface type denote significant snow events (defined as a snowfall of at least 25 cm at one or more first-order stations in the Northeast).

Onset date of Northeast precipitation event	Northeast precipitation anomaly (std dev)	Domain-averaged Northeast precipitation (mm)	NAO index (std dev)
14 Mar 1993	2.63	26.6	1.09
18 Jan 1994	2.60	19.1	1.85
10 Mar 1994	2.55	23.3	2.07
15 Jan 1999	2.51	16.8	2.15
21 Dec 1951*	2.50	19.6	1.97
18 Jan 1978	2.49	17.3	1.61
1 Feb 1951	2.47	19.4	1.83
7 Jan 1962	2.45	17.7	1.52
26 Feb 1979	2.40	18.4	1.12
9 Mar 1995	2.36	19.8	1.07
15 Mar 1986	2.35	20.4	1.97
17 Feb 1954	2.33	19.8	1.36
3 Mar 1994	2.30	18.9	1.55
11 Jan 1983	2.28	16.0	1.07
7 Feb 1951	2.27	14.3	1.28
7 Mar 1967*	2.27	20.1	1.74
27 Mar 1978	2.23	17.6	1.78
28 Nov 1959	2.21	23.6	1.89
24 Dec 1990*	2.18	15.6	2.83
5 Feb 1997	2.17	15.0	1.27
21 Nov 1986	2.16	19.0	2.09
1 Apr 1962**	2.16	22.3	1.02
24 Apr 1977	2.13	16.7	2.00
5 Jan 1993*	2.08	12.6	1.60
20 Jan 1978	2.05	12.0	1.47
16 Dec 1982	2.04	14.3	2.18
21 Feb 1989	2.04	14.2	2.01
28 Feb 1995	2.04	11.7	2.40
6 Jan 1962	2.03	12.0	1.11
14 Mar 1980	2.01	14.8	1.12

* Also occurring during a negative PNA regime.
** Also occurring during a positive PNA regime.

NAO regimes, four of the events are found to occur during negative PNA regimes, with one event occurring during a positive PNA regime. Five of the 30 events (17%) are considered significant snow events (Table 3), including the well-documented superstorm of 12–14 March 1993 (Caplan 1995; Huo et al. 1995; Uccellini et al. 1995; Bosart et al. 1996; Dickinson et al. 1997; Schultz et al. 1997) and the 19–21 January 1978 snowstorm (Kocin and Uccellini 2004, 484–492).

At 500 hPa, a region of statistically significant negative height anomalies is centered near southern Greenland (Fig. 6a). Farther south, a region of statistically significant positive height anomalies stretches across the western and central North Atlantic. The resulting low-over-high height dipole pattern yields a strong meridional height gradient near 50°N. Evidence of associated enhancement of the North Atlantic jet is seen in Fig. 6b, with 300-hPa winds in excess of 60 m s^{-1} located over eastern Canada. Implied quasigeostrophic (QG) forcing for ascent over the Northeast associated with the right-entrance region of this jet is supported by a 500-hPa upward motion maximum over the Northeast (Fig. 6b). Implied advection of cyclonic absolute vorticity by the thermal wind (Fig. 6c) is also consistent with the location of the upward motion maximum over the Northeast. A surface cyclone is located over the Northeast, approximately one-quarter wavelength downstream of a mid- and upper-level trough (Figs. 6a,b). Significant low-level moisture transport from the North Atlantic is implied over Nova Scotia and extreme eastern New England by the collocation of a low-level jet (LLJ) exit region with PW values in excess of 15 mm (Fig. 6d).

All 21 major 24-h cool-season Northeast precipitation events occurring during a negative NAO regime

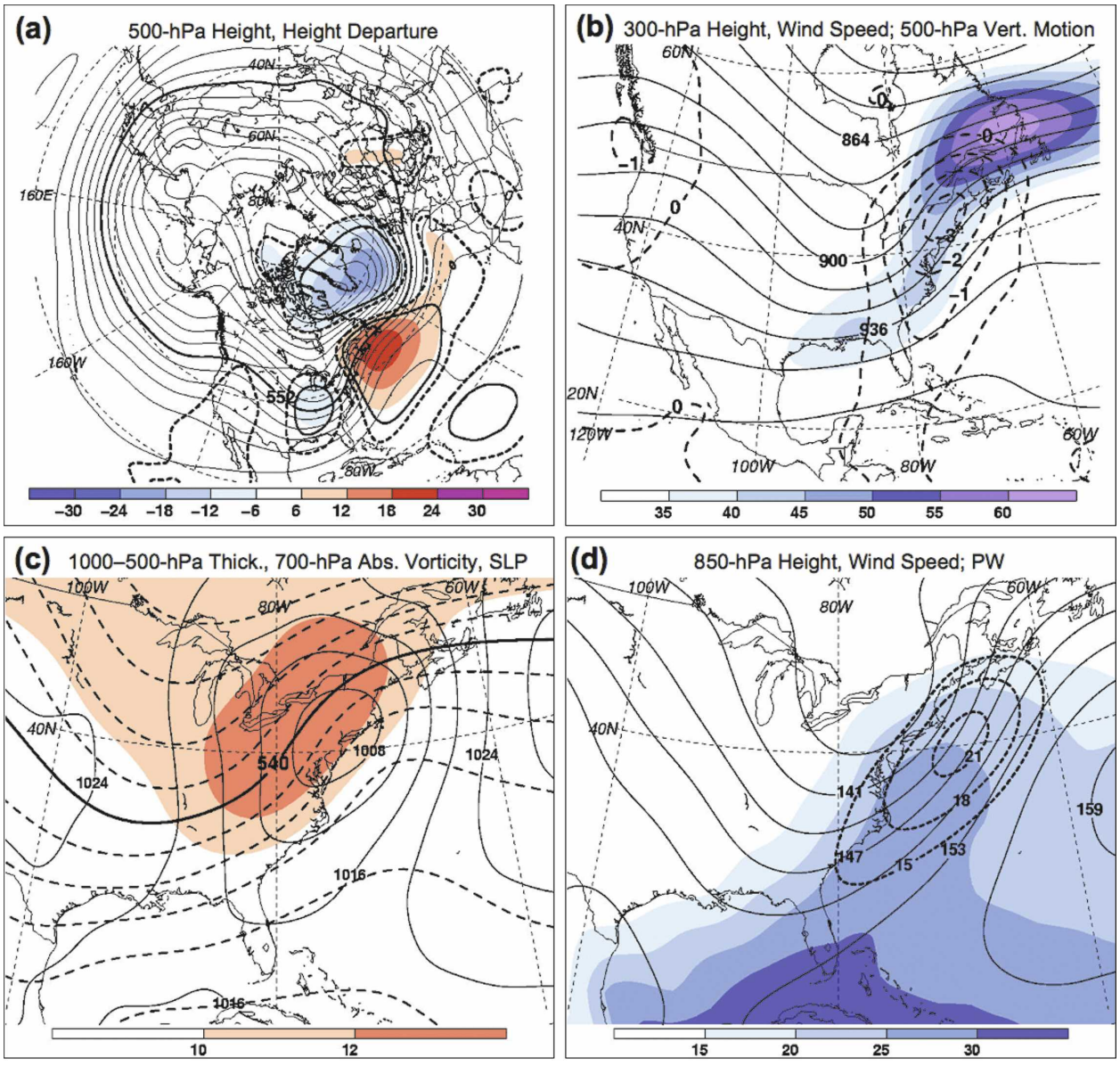

FIG. 6. Composite analyses of the onset of major 24-h cool-season Northeast precipitation events occurring during positive NAO regimes. Analyses show (a) 500-hPa geopotential height (solid; every 6 dam, with the 552-dam contour shown as a thick line) and departures from climatology (shaded; every 6 dam according to the color bar), where thick dashed (solid) contours denote regions where geopotential heights are significantly different from climatology at the 95% (99%) confidence level; (b) 300-hPa geopotential height (solid; every 12 dam), 300-hPa wind speed (shaded; beginning at 35 m s^{-1} according to the color bar), and 500-hPa vertical motion (dashed; every 1×10^{-3} hPa s^{-1}, zero and negative values only); (c) 1000–500-hPa thickness (dashed; every 6 dam, with the 540-dam contour shown as a thick line), 700-hPa absolute vorticity (shaded; beginning at 10×10^{-5} s^{-1} according to the color bar), and SLP (solid; every 4 hPa); and (d) 850-hPa geopotential height (solid; every 3 dam), 850-hPa wind speed (dashed; every 3 m s^{-1} beginning at 15 m s^{-1}), and PW (shaded; beginning at 15 mm according to the color bar).

are shown in Table 4. Three of these events also are found to occur during positive PNA regimes, and two are found to occur during negative PNA regimes. Seven events (33%), including the blizzard of 5–7 February 1978 (Kocin and Uccellini 2004, 494–503), are found to be significant snow events.

The composite 500-hPa height pattern for a negative NAO precipitation event (Fig. 7a) reveals a high-over-low height pattern over the central and eastern North Atlantic, which is indicative of blocked flow and a weakened North Atlantic jet stream relative to climatology. Further consideration of Fig. 7a reveals that a

TABLE 4. As in Table 3, but for the 21 major cool-season Northeast precipitation events occurring during negative NAO regimes.

Onset date of Northeast precipitation event	Northeast precipitation anomaly (std dev)	Domain-averaged Northeast precipitation (mm)	NAO index (std dev)
21 Jan 1979	2.79	27.7	−2.57
25 Dec 1978	2.62	21.7	−1.84
15 Nov 1995*	2.47	25.0	−1.93
19 Feb 1960	2.44	20.3	−1.29
4 Jan 1982**	2.39	17.4	−1.20
7 Nov 1963	2.37	28.9	−1.38
12 Nov 1995	2.36	26.7	−1.77
25 Jan 1979	2.22	19.4	−2.76
11 Feb 1960	2.21	13.9	−2.38
25 Mar 1969	2.16	18.1	−1.12
22 Jan 1958*	2.12	15.9	−1.99
22 Mar 2001	2.08	17.8	−1.03
6 Nov 1983	2.08	15.9	−2.07
28 Jan 1996**	2.07	14.3	−1.47
28 Dec 1968	2.07	14.4	−1.66
21 Nov 1952	2.06	17.2	−1.91
10 Nov 1990	2.04	20.6	−1.38
7 Feb 1978*	2.03	11.3	−1.19
30 Jan 1966	2.03	12.4	−1.05
22 Nov 1952	2.00	16.7	−1.88
8 Nov 1963	2.00	20.3	−1.88

* Also occurring during a positive PNA regime.
** Also occurring during a negative PNA regime.

region of statistically significant positive height anomalies centered over the Labrador Sea and southwestern Greenland extends southward to eastern Canada. The southward extension of the positive height anomalies is associated with a high-amplitude ridge over the western North Atlantic located downstream of a negatively tilted trough over the Ohio Valley and southeast United States (Figs. 7a,b). The relatively short distance between the trough axis and downstream ridge axis is suggestive of strong differential cyclonic vorticity advection and indicates ample QG forcing for ascent over the Northeast. The implied QG forcing for ascent is supported by a region of 500-hPa upward motion centered over the Northeast (Fig. 7b).

In contrast to the onset of positive NAO precipitation events, an upper-level jet streak is located over the southeast United States instead of eastern Canada at the onset of negative NAO precipitation events. This pattern places the left-exit region of a jet over the Northeast. The surface cyclone shown in Fig. 7c appears linked to stronger cyclonic vorticity advection by the thermal wind at the onset of negative NAO precipitation events compared with positive NAO precipitation events (Fig. 6c). The downstream thermal ridge associated with negative NAO precipitation events (Fig. 7c) is also greater in amplitude relative to the thermal ridge associated with positive NAO precipitation events (Fig. 6c). Another major difference between major cool-season Northeast precipitation events occurring during the two regimes is the location of the LLJ exit region farther westward over eastern New England at the onset of negative NAO events (cf. Figs. 7d and 6d). This pattern suggests that Atlantic moisture transport into the Northeast is more significant during negative NAO events than positive NAO events.

Composite plots of all major 24-h cool-season Northeast precipitation events occurring during positive PNA regimes (Table 5) are shown in Fig. 8. As noted above, three of these events also are found to occur during a negative NAO regime, including the blizzard of 5–7 February 1978 (Kocin and Uccellini 2004, 494–503), and one during a positive NAO regime. Six of the major cool-season precipitation events occurring during a positive PNA regime (23%) are significant snow events.

Inspection of the composite analyses of these precipitation events suggests that positive PNA precipitation events resemble negative NAO precipitation events more closely than positive NAO precipitation events. Although the mid- and upper-level trough upstream of the Northeast is more amplified for positive PNA precipitation events (Figs. 8a,b) than negative NAO precipitation events (Figs. 7a,b), a relatively high-amplitude mid- and upper-level ridge is situated over eastern Canada in both events (Figs. 7a,b and 8a,b). Additionally, a surface cyclone is located over the Northeast (Fig. 8c), and an upper-level jet streak is situated over the southeast United States at the onset of positive PNA events, placing the left-exit region of a jet streak above the Northeast (Fig. 8b). In contrast to negative NAO precipitation events, on the other hand, a right-entrance region of a jet streak over eastern Canada is also located over the Northeast (Fig. 8b). As is the case for the onset of positive and negative NAO precipitation events, QG forcing for ascent over the Northeast, implied by cyclonic absolute vorticity advection by the thermal wind (Fig. 8c), is accompanied by 500-hPa upward motion over the Northeast (Fig. 8b). At lower levels, a jet exit region collocated with PW values exceeding 15 mm over northeastern New England and the Gulf of Maine implies strong moisture transport there (Fig. 8d).

Composite analyses of the onset of all negative PNA major precipitation events (shown in Table 6) are displayed in Fig. 9. As mentioned above, four of the precipitation events are also found to occur during positive NAO regimes, and two events are during the negative

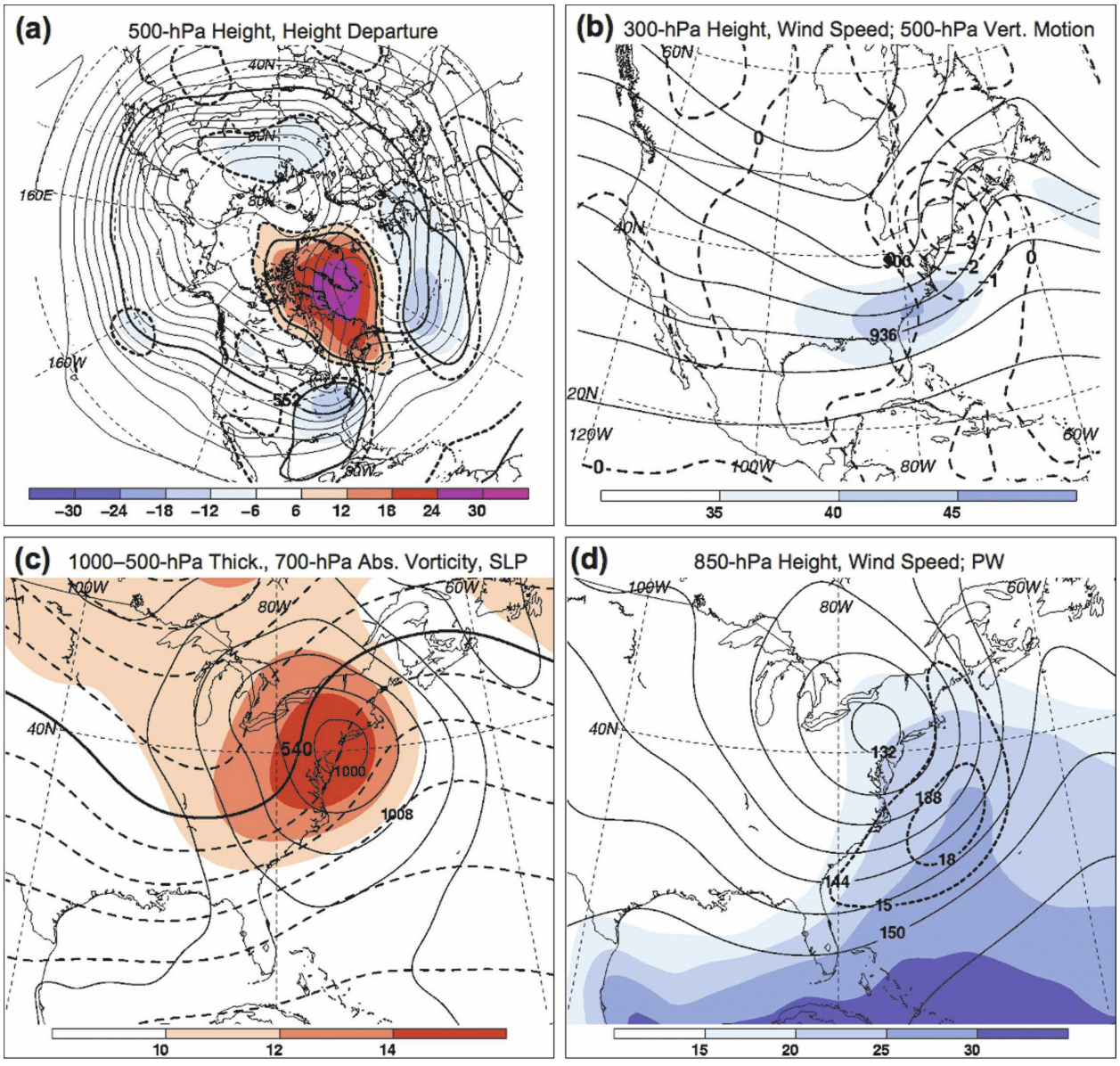

FIG. 7. As in Fig. 6, but for the onset of major 24-h cool-season Northeast precipitation events occurring during negative NAO regimes.

NAO regimes. Of the 27 major precipitation events, 7 are categorized as significant snow events (26%).

As is characteristic of a negative PNA regime, the mid- and upper-level height pattern (Figs. 9a,b) over North America and the North Atlantic is relatively zonal. A weak shortwave trough approaching the Northeast is embedded within a broader trough over Canada and the northern United States. As with the three other types of Northeast precipitation events, a ridge is located downstream of the Northeast over the western North Atlantic and eastern Canada (Figs. 9a,b). This downstream ridge, however, is less amplified than for the other three types of Northeast precipitation events (Figs. 6a,b, 7a,b, and 8a,b). The thermal ridge associated with the negative PNA events is also comparatively lower in amplitude (cf. Fig. 9c with Figs. 6c, 7c, and 8c). Two upper-level jet streaks are apparent at the onset of negative PNA precipitation events—one over the Missouri and lower Ohio Valleys and a second over eastern Canada (Fig. 9b). Thus, like positive PNA precipitation events, a right-entrance region and a left-exit region of a jet are both located over the Northeast at the onset of negative PNA precipitation events (Fig. 9b). A surface cyclone (Fig. 9c) and area of 500-hPa

TABLE 5. As in Table 3, but for the 26 major cool-season Northeast precipitation events occurring during positive PNA regimes.

Onset date of Northeast precipitation event	Northeast precipitation anomaly (std dev)	Domain-averaged Northeast precipitation (mm)	PNA index (std dev)
21 Dec 1973	2.97	29.0	1.44
26 Dec 1975	2.68	22.5	1.33
15 Nov 1995*	2.47	25.0	2.58
30 Nov 1963	2.44	24.1	2.45
17 Dec 1973	2.39	19.2	1.53
18 Dec 2003	2.30	18.0	1.10
25 Dec 1986	2.28	16.1	1.53
11 Feb 1970	2.25	14.4	1.57
15 Jan 1958	2.25	13.2	1.83
2 Jan 2003	2.21	16.4	1.75
1 Apr 1962**	2.16	22.3	1.76
2 Nov 1997	2.16	22.6	1.25
11 Mar 1992	2.15	16.7	2.15
31 Mar 1987	2.14	19.6	1.16
22 Jan 1958*	2.12	15.9	1.43
22 Dec 1969	2.12	13.8	2.16
30 Nov 1987	2.08	17.1	2.08
16 Nov 1983	2.08	15.9	2.01
10 Mar 1998	2.06	14.7	1.48
18 Feb 1998	2.05	14.0	2.00
2 Dec 1974	2.03	16.8	1.71
7 Feb 1978*	2.03	11.3	2.00
21 Nov 1954	2.02	16.5	3.12
16 Jan 1998	2.02	10.5	1.53
21 Jan 1995	2.02	13.4	1.68
24 Jan 1998	2.01	15.5	1.48

* Also occurring during a negative NAO regime.
** Also occurring during a positive NAO regime.

upward motion (Fig. 9b) are positioned near a region of comparatively weak cyclonic vorticity advection by the thermal wind over the Northeast (Fig. 9c). Finally, the most significant low-level moisture transport appears to remain offshore: the LLJ exit region is located primarily over the western North Atlantic rather than over the Northeast (Fig. 9d).

5. Discussion

a. Statistical analysis interpretation

Results of a statistical analysis of cool-season Northeast precipitation for the period 1948–2003 indicate that PNA regimes influence cool-season Northeast precipitation amount and frequency more significantly than do NAO regimes, likely because the PNA domain is located upstream, rather than downstream, of the Northeast. The findings that cool-season Northeast precipitation is enhanced during negative PNA regimes and suppressed during positive PNA regimes (Figs. 3 and 4; Table 2) are consistent with previous findings that the phase of the PNA pattern and precipitation in parts of the Northeast and Ohio Valley is negatively correlated (Leathers et al. 1991; Notaro et al. 2006). Additionally, results indicating that light and moderate cool-season Northeast precipitation events are more likely during negative PNA regimes and less likely during positive PNA regimes compared to the overall cool-season climatology (Figs. 4e–h) suggest that Northeast precipitation associated with frontal passages is more frequent or heavier during relatively zonal negative PNA regimes and less frequent or lighter during relatively meridional positive PNA regimes. These associations are supported by previous findings that Northeast frontal passages are relatively frequent during negative PNA phases and relatively infrequent during positive PNA phases (Notaro et al. 2006).

Major cool-season Northeast precipitation events are found to occur slightly more frequently during positive NAO regimes and slightly less frequently during negative NAO regimes compared to climatology (Fig. 4a–d). Additionally, a tendency is noted for the phase of the NAO to be positive during extreme cool-season Northeast precipitation events (Fig. 5). These statistical relationships suggest that extreme cool-season Northeast precipitation occurring during the positive phase of the NAO may be enhanced by the ascending branch of an ageostrophic circulation associated with the entrance region of an anomalously strong North Atlantic jet.

The result that the positive NAO–negative PNA combination regime is the wettest cool-season regime for the Northeast is consistent with previous findings that frontal passages occur more frequently during a positive NAO–negative PNA pattern than any other regime (Notaro et al. 2006). The finding that the negative NAO–positive PNA regime is the driest cool-season regime for the Northeast may be counterintuitive, given "conventional wisdom" holding that this large-scale pattern is the most favorable pattern for Northeast snowstorms. It is speculated, however, that if Northeast snowstorms are indeed more frequent during negative NAO–positive PNA regimes, it is primarily because any precipitation is more likely to fall as snow because of colder conditions associated with a negative NAO and a positive PNA pattern (e.g., Notaro et al. 2006).

Although cool-season Northeast precipitation anomalies associated with individual PNA regimes are found to be statistically significant, the magnitudes of all precipitation anomalies associated with the large-scale regimes examined in this study are relatively small. This result may be explained as follows. First, the factors influencing cool-season precipitation vary

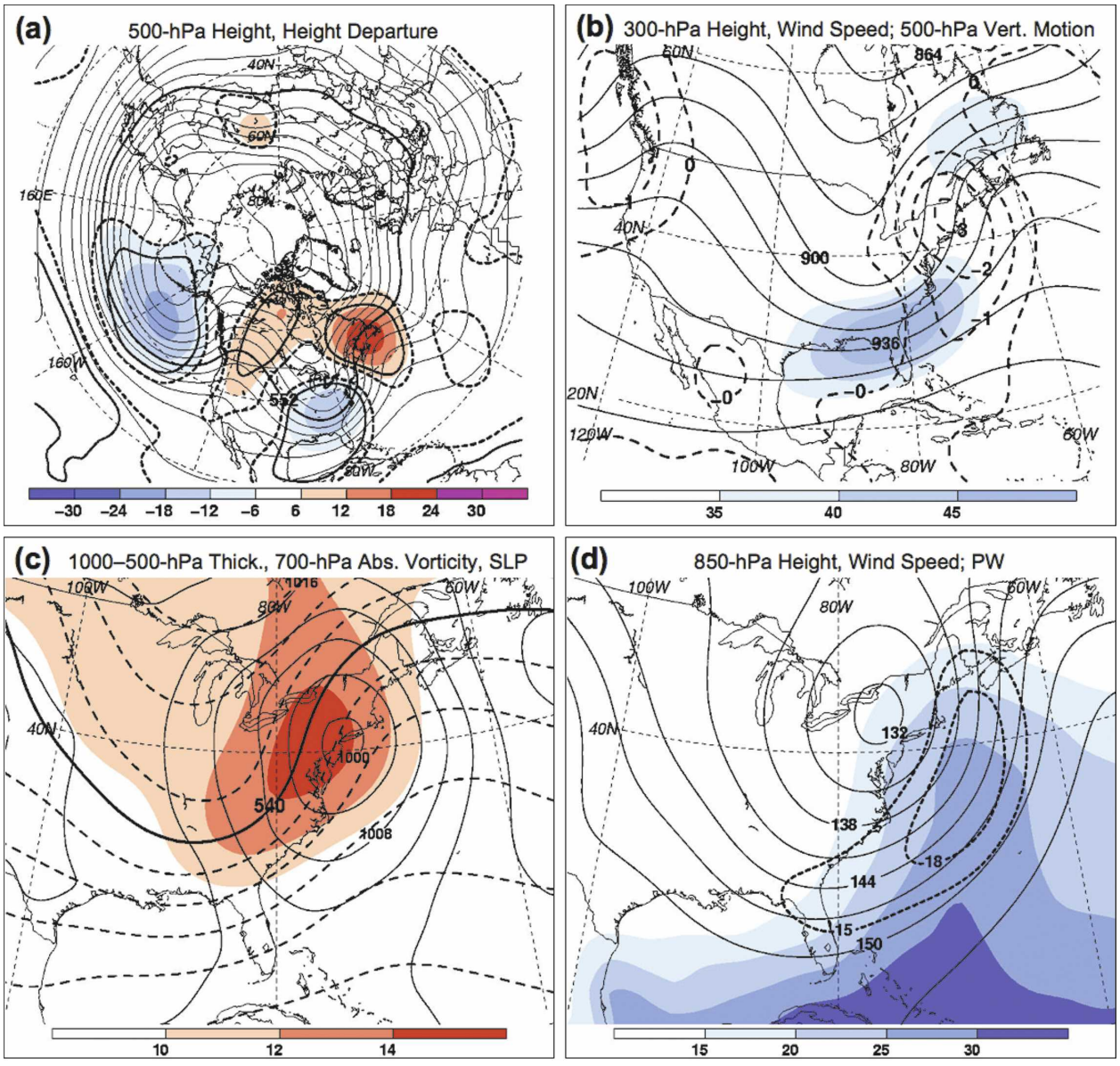

FIG. 8. As in Fig. 6, but for the onset of major 24-h cool-season Northeast precipitation events occurring during positive PNA regimes.

across the Northeast. Lake-effect precipitation has a substantial influence on total cool-season precipitation in regions close to the Great Lakes, and is likely a major reason that moderate precipitation events tend to occur more frequently across northwest sections of the Northeast compared to southeastern sections (Wagner 2006). Additionally, the influence of the PNA pattern on cool-season precipitation is found to increase westward from the Northeast to the Ohio Valley (e.g., Leathers et al. 1991), whereas the influence of the NAO on cool-season precipitation is found to increase southeastward from the Northeast to the western Atlantic (Hurrell 1995).

The second possible reason that cool-season precipitation anomalies associated with large-scale regimes are found to be relatively small is related to the strong modulation of cool-season precipitation by the storm track, which suggests that even small storm-track variations may produce dramatically different precipitation distributions. For example, analyses of the 25 January 2000 "surprise" East Coast snowstorm (e.g., Langland et al. 2002; Zhang et al. 2002) demonstrate that a slight

TABLE 6. As in Table 3, but for the 27 major cool-season Northeast precipitation events occurring during negative PNA regimes.

Onset date of Northeast precipitation event	Northeast precipitation anomaly (std dev)	Domain-averaged Northeast precipitation (mm)	PNA index (std dev)
30 Jan 1990	2.58	20.8	−1.44
8 Feb 1965	2.57	17.9	−1.67
20 Nov 2003	2.55	29.8	−1.26
21 Dec 1951*	2.50	19.6	−1.33
4 Jan 1982**	2.39	17.4	−1.07
20 Jan 1996	2.39	16.5	−1.08
13 Feb 1966	2.32	17.1	−1.27
24 Feb 1962	2.28	17.4	−2.29
4 Mar 1971	2.28	20.4	−1.03
7 Mar 1967*	2.27	21.0	−1.49
10 Feb 1959	2.23	14.0	−2.53
14 Mar 1977	2.19	17.6	−1.86
29 Dec 1967	2.18	16.0	−1.03
24 Dec 1990*	2.18	15.6	−2.03
13 Mar 1977	2.18	16.7	−1.41
17 Dec 1970	2.16	15.5	−1.19
22 Dec 1983	2.15	14.3	−1.92
10 Mar 1964	2.14	15.9	−1.50
1 Mar 1955	2.11	12.0	−2.40
9 Feb 1994	2.08	11.5	−2.17
5 Jan 1993*	2.08	12.6	−1.98
28 Jan 1996**	2.07	14.3	−1.24
14 Feb 1966	2.06	14.1	−1.82
12 Mar 1985	2.06	15.4	−1.13
8 Mar 1956	2.06	16.1	−1.46
17 Mar 1973	2.06	15.8	−1.21
11 Jan 2000	2.02	12.5	−1.66

* Also occurring during a positive NAO regime.
** Also occurring during a negative NAO regime.

shift in the actual surface cyclone track relative to the model-forecast surface cyclone tracks can result in unanticipated, widespread heavy snowfall. Third, the spatial distribution and intensity of precipitation during cool-season precipitation events are often strongly influenced by mesoscale features, such as gravity waves and banding associated with frontogenesis (e.g., Bosart et al. 1998; Roebber and Bosart 1998; Nicosia and Grumm 1999; Novak et al. 2004, 2006), which tend to correlate poorly with the large-scale flow pattern. Finally, when relationships do exist between mesoscale precipitation and large-scale regimes, they may act in opposition to the large-scale regime–synoptic-scale precipitation relationships that presumably are responsible for the coherence of the statistical large-scale regime/cool-season precipitation relationships documented in this and other studies. A prime example of a mesoscale precipitation–large-scale regime relationship is the tendency for lake-effect snow to be enhanced over the Northeast when a relatively cold and otherwise dry negative NAO–positive PNA pattern is in place (Notaro et al. 2006).

A significant difference between the present study and many past studies on the statistical relationships between the NAO and PNA pattern and cool-season precipitation (e.g., Leathers et al. 1991; Hurrell 1995; Serreze et al. 1998; Coleman and Rogers 2003) is our use of daily, rather than monthly, teleconnection index values to identify NAO and PNA regimes. Despite this difference in methodology, the relationships between cool-season NAO and PNA regimes and Northeast precipitation presented in our study are consistent with those documented elsewhere. The consistency of the results of the present study with those of previous studies suggests that the relationships between NAO and PNA regimes and cool-season Northeast precipitation documented in the present study are valid on both synoptic and intraseasonal time scales.

b. Composite analysis interpretation

The coherence of the synoptic-scale patterns shown in the composite analyses of major cool-season Northeast precipitation events (Figs. 6–9) is noteworthy given that the selection criteria for events in the composite analyses do not include the stipulation that any distinct synoptic-scale feature, such as a surface cyclone, be present. Schematics of the synoptic- and large-scale patterns associated with the onset of major cool-season Northeast precipitation events during various regimes (Fig. 10) reveal that a surface cyclone over the Northeast, flanked by an upstream trough over the Ohio Valley and a downstream ridge over eastern Canada at 500 hPa, is a signature of all four types of major cool-season Northeast precipitation events. Upper- and lower-level jets in the vicinity of the Northeast are also found to be signatures of major cool-season Northeast precipitation events.

The overall synoptic pattern associated with major cool-season Northeast precipitation events found in this study corroborates results of other observational studies. Sisson and Gyakum (2004) noted that an upstream 500-hPa trough, surface cyclone, and downstream 500-hPa ridge tend to be observed during heavy cool-season precipitation events in the Northeast, and Sanders and Davis (1988) and Bell and Bosart (1989) identified a similar flow pattern associated with Atlantic coastal cyclogenesis events.

Although some similarities exist between major cool-season Northeast precipitation events occurring during the four large-scale regimes examined in this study, the synoptic signatures of major cool-season Northeast precipitation events are found to be strongly dependent upon the governing large-scale flow. Negative NAO

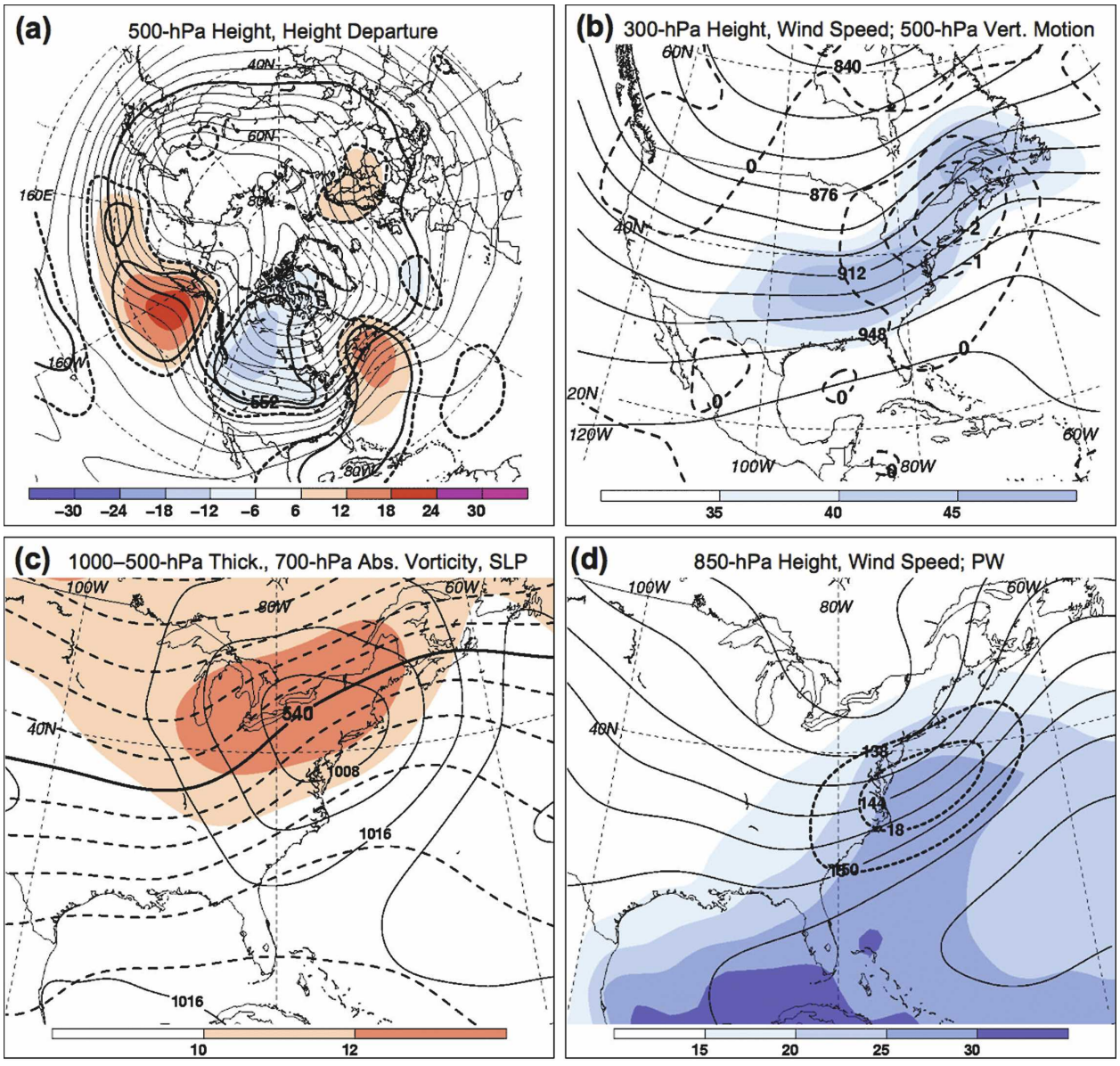

FIG. 9. As in Fig. 6, but for the onset of major 24-h cool-season Northeast precipitation events occurring during negative PNA regimes.

and positive PNA major precipitation events tend to be accompanied by a highly amplified trough–ridge pattern (Figs. 10b,c). In contrast, during positive NAO and negative PNA precipitation events, the amplitude of the trough–ridge pattern is moderate and low, respectively (Figs. 10a,d). The highly amplified flow accompanying major cool-season Northeast precipitation events during negative NAO and positive PNA regimes suggests that forcing for ascent during these events may be primarily attributed to strong differential cyclonic vorticity advection rather than a relative maximum of warm-air advection over the Northeast. Conversely, the less amplified flow associated with major cool-season Northeast precipitation events during positive NAO and negative PNA regimes suggests that forcing for ascent during such events may be primarily attributed to a relative maximum of warm-air advection rather than to strong differential cyclonic vorticity advection over the Northeast.

The upper-level jet structure associated with major cool-season Northeast precipitation events, and thus, the potential role of ageostrophic circulations associated with jet entrance and exit regions, is found to vary with the governing large-scale flow regime. During

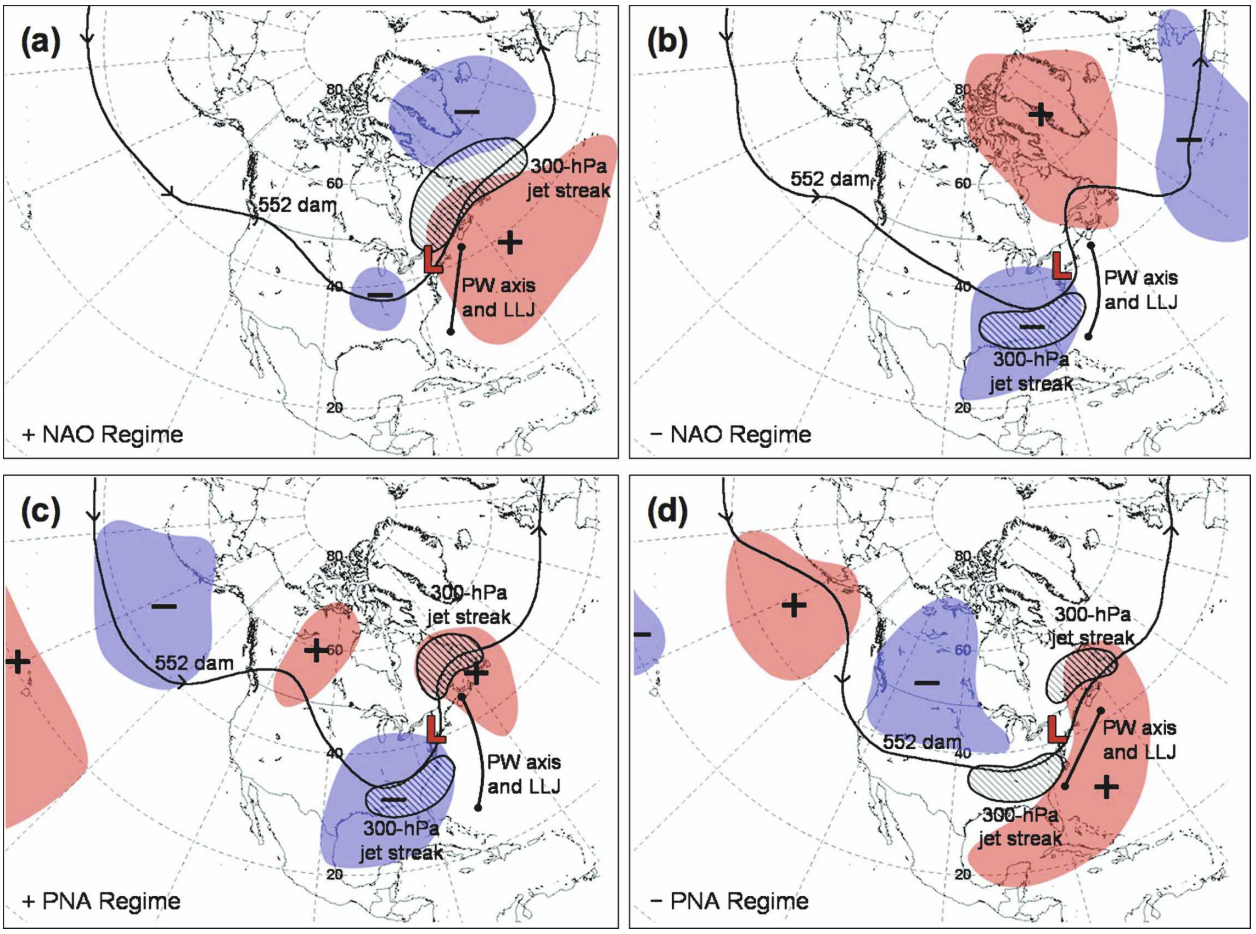

FIG. 10. Synoptic-scale patterns for the onset of major 24-h cool-season Northeast precipitation events occurring during (a) positive NAO, (b) negative NAO, (c) positive PNA, and (d) negative PNA regimes. Shading indicates mean locations of 500-hPa geopotential height departures from climatology found to be statistically significant at the 99% confidence level, with red (blue) shading denoting positive (negative) geopotential height anomalies. The "L" symbol indicates the mean position of the surface cyclone center. The solid black line denotes the mean position of the 552-dam geopotential height contour. Hatching indicates the mean locations of 300-hPa jet streaks, whereas the line segment denotes the mean position of the PW axis and 850-hPa LLJ.

positive and negative PNA major precipitation events (Fig. 10c,d), both the right-entrance and left-exit regions of the jets tend to be located over the Northeast, suggesting that upward motion over the Northeast during these events may be enhanced by ascending branches of both thermally direct and thermally indirect circulations. This lateral upper-level jet coupling has been identified as a common signature of major Northeast snowstorms (Uccellini and Kocin 1987), as well as oceanic cyclones occurring near the eastern U.S. coast (e.g., Rogers and Bosart 1991).

During positive NAO major precipitation events, only the right-entrance region of a jet tends to be positioned over the Northeast (Fig. 10a), implying that the ascending branch of a thermally direct ageostrophic circulation enhances upward motion over the Northeast during these precipitation events. It is interesting to note that, although shearing deformation associated with a strong North Atlantic jet may sometimes mitigate cyclone activity and associated heavy precipitation in the Northeast, the presence of a strong North Atlantic jet can favor Northeast cyclone activity and precipitation as long as the jet is positioned such that its right-entrance region is in close proximity to the Northeast. In contrast to positive NAO events, the signature of a left-exit region of a jet over the Northeast during negative NAO precipitation events (Fig. 10b) implies that the ascending branch of a thermally indirect ageostrophic circulation enhances upward motion during these events.

Different PW axis and LLJ orientations are found for major cool-season Northeast precipitation events occurring during different large-scale regimes. During negative NAO and positive PNA precipitation events,

the PW axis and LLJ bend toward the Northeast from the western North Atlantic (Figs. 10b,c), whereas during positive NAO and negative PNA regimes, the PW axis and LLJ are oriented more offshore (Figs. 10a,d). Thus, more substantial meridional moisture transport into the Northeast is implied by the orientation of the PW axis and LLJ during negative NAO and positive PNA precipitation events than during positive NAO and negative PNA precipitation events.

Although the synoptic portion of this study focuses only on the onset of major cool-season Northeast precipitation events, it is possible to infer differences in tracks and moisture sources of the associated surface cyclones leading up to the major cool-season Northeast precipitation events. The relatively zonal large-scale flow pattern associated with the onset of positive NAO and negative PNA major precipitation events (Figs. 10a,d) suggests that associated surface cyclones would originate from the west or southwest over the Great Lakes or Tennessee Valley regions and track eastward or northeastward toward the Northeast. Support for a generally west-to-east cyclone track is lent by studies indicating that cyclones impacting the Great Lakes tend to exhibit an eastward or northeastward track during the negative phase of the PNA pattern (Rodionov 1994; Isard et al. 2000). Such a cyclone track implies that the primary moisture sources for surface cyclones producing major cool-season Northeast precipitation events during positive NAO and negative PNA regimes initially would be the Gulf of Mexico and the Great Lakes.

In contrast, the relatively meridional large-scale flow associated with the onset of negative NAO and positive PNA major precipitation events (Figs. 10b,c) suggests that the associated surface cyclones would either originate from Canada and exhibit a southeastward track [an "Alberta clipper" track; e.g., Thomas and Martin (2007)], or originate farther south over the southeastern United States and exhibit a northward or northeastward track. Studies have indicated that cyclones impacting the Great Lakes during the positive phases of the PNA tend to be Alberta clipper–type cyclones (Rodionov 1994; Isard et al. 2000). The propensity for intrusions of cold, dry air over the eastern United States during negative NAO and positive PNA patterns (e.g., Leathers et al. 1991; Notaro et al. 2006) would likely rule out the Gulf of Mexico as an important moisture source for surface cyclones producing major cool-season Northeast precipitation events during negative NAO and positive PNA regimes. Instead, the Great Lakes would likely provide the primary initial moisture source to cyclones tracking southeastward from Canada toward the Northeast, whereas the western Atlantic would likely be the primary moisture source for cyclones tracking north or northeastward from the southeastern United States toward the Northeast.

6. Summary

The present study investigates the influence of recurrent large-scale flow regimes on cool-season Northeast precipitation from statistical and synoptic perspectives. NAO and PNA regimes occurring between 1948 and 2003 are objectively identified using daily NAO and PNA index time series created from twice-daily NCEP–NCAR reanalysis 500-hPa geopotential height grids. Cool-season (November–April) Northeast precipitation during NAO and PNA regimes is analyzed using data obtained from the NCEP Unified Precipitation Dataset, and synoptic patterns of major (two standard deviation) 24-h cool-season Northeast precipitation events occurring during the regimes are examined using composite analyses generated from the NCEP–NCAR reanalysis.

Results of the statistical analysis reveal that positive and negative PNA regimes are associated with statistically significant cool-season Northeast precipitation anomalies, whereas positive and negative NAO regimes are not. Negative PNA regimes are associated with above-average cool-season Northeast precipitation and an increased frequency of light and moderate cool-season precipitation events. Conversely, positive PNA regimes are associated with below-average cool-season Northeast precipitation and a decreased frequency of light and moderate cool-season precipitation events. A tendency for the phases of the NAO and the PNA patterns to be positive during extreme cool-season Northeast precipitation events is also noted.

The synoptic analysis of the onset of major 24-h cool-season Northeast precipitation events during the four types of individual large-scale flow regimes indicates that major Northeast precipitation events generally are characterized by (i) a surface cyclone flanked by an upstream trough over the Ohio Valley and downstream ridge over eastern Canada, (ii) one or more distinct upper-level jet streaks in close proximity to the Northeast, and (iii) implied moisture transport associated with a distinct LLJ. Differences in major cool-season Northeast precipitation events identified in this study include (i) a more amplified upstream ridge and downstream trough associated with negative NAO and positive PNA major precipitation events, (ii) a signal of lateral jet coupling during negative and positive PNA major precipitation events only, and (iii) greater Atlantic moisture transport into the Northeast implied by an

LLJ with a stronger onshore component during negative NAO and positive PNA major precipitation events.

Acknowledgments. The authors are grateful for the insightful and constructive recommendations provided by Dr. Michael Notaro and two anonymous reviewers. Thanks are given to Kevin Tyle and Dr. David Knight at the University at Albany, SUNY, for providing technical support for this research. This work is based upon a portion of the first author's M.S. thesis at the University at Albany, SUNY, and was supported by NOAA Grant NA07WA0458 and National Science Foundation Grant ATM-0434189.

REFERENCES

Ambaum, M. H. P., B. J. Hoskins, and D. B. Stephenson, 2001: Arctic Oscillation or North Atlantic Oscillation? *J. Climate,* **14,** 3495–3507.

Barnston, A. G., and R. E. Livezey, 1987: Classification, seasonality and persistence of low-frequency atmospheric circulation patterns. *Mon. Wea. Rev.,* **115,** 1083–1126.

Bell, G. D., and L. F. Bosart, 1989: The large-scale atmospheric structure accompanying New England coastal frontogenesis and associated North American east coast cyclogenesis. *Quart. J. Roy. Meteor. Soc.,* **115,** 1133–1146.

Bosart, L. F., G. J. Hakim, K. R. Tyle, M. A. Bedrick, W. E. Bracken, M. J. Dickinson, and D. M. Schultz, 1996: Large-scale antecedent conditions associated with the 12–14 March 1993 cyclone ("superstorm '93") over eastern North America. *Mon. Wea. Rev.,* **124,** 1865–1891.

——, W. E. Bracken, and A. Seimon, 1998: A study of cyclone mesoscale structure with emphasis on a large-amplitude inertia–gravity wave. *Mon. Wea. Rev.,* **126,** 1497–1527.

Branstator, G., 1995: Organization of storm track anomalies by recurring low-frequency circulation anomalies. *J. Atmos. Sci.,* **52,** 207–226.

Caplan, P. M., 1995: The 12–14 March 1993 superstorm: Performance of NCEP global medium range model. *Bull. Amer. Meteor. Soc.,* **76,** 201–212.

Coleman, J. S., and J. C. Rogers, 2003: Ohio River valley winter moisture conditions associated with the Pacific–North American teleconnection pattern. *J. Climate,* **16,** 969–981.

Deser, C., 2000: On the teleconnectivity of the "Arctic Oscillation." *Geophys. Res. Lett.,* **27,** 779–782.

Dickinson, M. J., L. F. Bosart, W. E. Bracken, G. J. Hakim, D. M. Schultz, M. A. Bedrick, and K. R. Tyle, 1997: The March 1993 superstorm: Incipient phase synoptic- and convective-scale flow interaction and model performance. *Mon. Wea. Rev.,* **125,** 3041–3072.

Dole, R. M., 1986: Persistent anomalies of the extratropical Northern Hemisphere wintertime circulation: Structure. *Mon. Wea. Rev.,* **114,** 178–207.

——, and N. D. Gordon, 1983: Persistent anomalies of the extratropical Northern Hemisphere wintertime circulation: Geographical distribution and regional persistence characteristics. *Mon. Wea. Rev.,* **111,** 1567–1586.

Feldstein, S. B., 2002: Fundamental mechanisms of the growth and decay of the PNA teleconnection pattern. *Quart. J. Roy. Meteor. Soc.,* **128,** 775–796.

——, 2003: The dynamics of NAO teleconnection pattern growth and decay. *Quart. J. Roy. Meteor. Soc.,* **129,** 901–924.

——, and C. Franzke, 2006: Are the North Atlantic Oscillation and the Northern Annular Mode distinguishable? *J. Atmos. Sci.,* **63,** 2915–2930.

Higgins, R. W., W. Shi, E. Yarosh, and R. Joyce, 2000: *Improved United States Precipitation Quality Control System and Analysis.* NCEP/Climate Prediction Center Atlas 7, 45 pp. [Available online at http://www.cpc.ncep.noaa.gov/research_papers/ncep_cpc_atlas/7/index.html.]

Huo, Z., D.-L. Zhang, J. R. Gyakum, and A. Staniforth, 1995: A diagnostic analysis of the superstorm of March 1993. *Mon. Wea. Rev.,* **123,** 1740–1761.

Hurrell, J. W., 1995: Decadal trends in the North Atlantic Oscillation: Regional temperatures and precipitation. *Science,* **269,** 676–679.

Isard, S. A., J. R. Angel, and G. T. VanDyke, 2000: Zones of origin for Great Lakes cyclones in North America, 1899–1996. *Mon. Wea. Rev.,* **128,** 474–485.

Johansson, Å., 2007: Prediction skill of the NAO and PNA from daily to seasonal time scales. *J. Climate,* **20,** 1957–1975.

Kalnay, E., and Coauthors, 1996: The NCEP/NCAR 40-Year Reanalysis Project. *Bull. Amer. Meteor. Soc.,* **77,** 437–471.

Kistler, R., and Coauthors, 2001: The NCEP–NCAR 50-Year Reanalysis: Monthly means CD-ROM and documentation. *Bull. Amer. Meteor. Soc.,* **82,** 247–267.

Kocin, P. J., and L. W. Uccellini, 2004: *Northeast Snowstorms (Volume I: Overview, Volume II: The Cases). Meteor. Monogr.,* No. 54, Amer. Meteor. Soc., 818 pp.

Lackmann, G. M., L. F. Bosart, and D. Keyser, 1996: Planetary- and synoptic-scale characteristics of explosive wintertime cyclogenesis over the western North Atlantic Ocean. *Mon. Wea. Rev.,* **124,** 2672–2702.

Langland, R. H., M. A. Shapiro, and R. Gelaro, 2002: Initial condition sensitivity and error growth in forecasts of the 25 January 2000 East Coast snowstorm. *Mon. Wea. Rev.,* **130,** 957–974.

Leathers, D. J., B. Yarnal, and M. A. Palecki, 1991: The Pacific/North American teleconnection pattern and United States climate. Part I: Regional temperature and precipitation associations. *J. Climate,* **4,** 517–528.

Namias, J., 1950: The index cycle and its role in the general circulation. *J. Meteor.,* **7,** 130–139.

Nicosia, D. J., and R. H. Grumm, 1999: Mesoscale band formation in three major northeastern United States snowstorms. *Wea. Forecasting,* **14,** 346–368.

Notaro, M., W.-C. Wang, and W. Gong, 2006: Model and observational analysis of the northeast U.S. regional climate and its relationship to the PNA and NAO patterns during early winter. *Mon. Wea. Rev.,* **134,** 3479–3505.

Novak, D. R., L. F. Bosart, D. Keyser, and J. S. Waldstreicher, 2004: An observational study of cold season–banded precipitation in northeast U.S. cyclones. *Wea. Forecasting,* **19,** 993–1010.

——, J. S. Waldstreicher, D. Keyser, and L. F. Bosart, 2006: A forecast strategy for anticipating cold season mesoscale band formation within eastern U.S. cyclones. *Wea. Forecasting,* **21,** 3–23.

Pelly, J. L., and B. J. Hoskins, 2003: A new perspective on blocking. *J. Atmos. Sci.,* **60,** 743–755.

Quadrelli, R., and J. M. Wallace, 2004: A simplified linear framework for interpreting patterns of Northern Hemisphere wintertime climate variability. *J. Climate,* **17,** 3728–3744.

Rex, D. F., 1950a: Blocking action in the middle troposphere and its effects upon regional climate I. An aerological study of blocking action. *Tellus,* **2,** 196–211.

——, 1950b: Blocking action in the middle troposphere and its effects upon regional climate II. The climatology of blocking action. *Tellus,* **2,** 275–301.

Rodionov, S. N., 1994: Association between winter precipitation and water level fluctuations in the Great Lakes and atmospheric circulation patterns. *J. Climate,* **7,** 1693–1706.

Roebber, P. J., and L. F. Bosart, 1998: The sensitivity of precipitation to circulation details. Part I: An analysis of regional analogs. *Mon. Wea. Rev.,* **126,** 437–455.

Rogers, E., and L. F. Bosart, 1991: A diagnostic study of two intense oceanic cyclones. *Mon. Wea. Rev.,* **119,** 965–996.

Rogers, J. C., 1990: Patterns of low-frequency monthly sea level pressure variability (1899–1986) and associated wave cyclone frequencies. *J. Climate,* **3,** 1364–1379.

Rossby, C.-G., 1939: Relation between variations in the intensity of the zonal circulation of the atmosphere and the displacements of the semi-permanent centers of action. *J. Mar. Res.,* **2,** 38–55.

——, and H. C. Willett, 1948: The circulation of the upper troposphere and lower stratosphere. *Science,* **108,** 643–652.

Sanders, F., and C. A. Davis, 1988: Patterns of thickness anomaly for explosive cyclogenesis over the west-central North Atlantic Ocean. *Mon. Wea. Rev.,* **116,** 2725–2730.

Schultz, D. M., W. E. Bracken, L. F. Bosart, G. J. Hakim, M. A. Bedrick, M. J. Dickinson, and K. R. Tyle, 1997: The 1993 superstorm cold surge: Frontal structure, gap flow, and tropical impact. *Mon. Wea. Rev.,* **125,** 5–39.

Serreze, M. C., M. P. Clark, D. A. Robinson, and D. L. McGinnis, 1998: Characteristics of snowfall over the eastern half of the United States and relationships with principal modes of low-frequency atmospheric variability. *J. Climate,* **11,** 234–250.

Sisson, P. A., and J. R. Gyakum, 2004: Synoptic-scale precursors to significant cold-season precipitation events in Burlington, Vermont. *Wea. Forecasting,* **19,** 841–854.

Thomas, B. C., and J. E. Martin, 2007: A synoptic climatology and composite analysis of the Alberta Clipper. *Wea. Forecasting,* **22,** 315–333.

Thompson, D. W., and J. M. Wallace, 1998: The Arctic Oscillation signature in the wintertime geopotential height and temperature fields. *Geophys. Res. Lett.,* **25,** 1297–1300.

——, and ——, 2000: Annular modes in the extratropical circulation. Part I: Month-to-month variability. *J. Climate,* **13,** 1000–1016.

Uccellini, L. W., and P. J. Kocin, 1987: The interaction of jet streak circulations during heavy snow events along the east coast of the United States. *Wea. Forecasting,* **2,** 289–308.

——, ——, R. S. Schneider, P. M. Stokols, and R. A. Dorr, 1995: Forecasting the 12–14 March 1993 superstorm. *Bull. Amer. Meteor. Soc.,* **76,** 183–199.

Wagner, K. R., 2006: Cool-season moderate precipitation events in the northeastern United States. M.S. thesis, Dept. of Earth and Atmospheric Sciences, University at Albany, State University of New York, 134 pp.

Walker, G. T., and E. W. Bliss, 1932: World Weather V. *Mem. Roy. Meteor. Soc.,* **44,** 53–84.

Wallace, J. M., 2000: North Atlantic Oscillation/annular mode: Two paradigms—One phenomenon. *Quart. J. Roy. Meteor. Soc.,* **126,** 791–805.

——, and D. S. Gutzler, 1981: Teleconnections in the geopotential height field during the Northern Hemisphere winter. *Mon. Wea. Rev.,* **109,** 784–812.

Wilks, D. S., 2006: *Statistical Methods in the Atmospheric Sciences.* 2nd ed. Academic Press, 627 pp.

Zhang, F., C. Snyder, and R. Rotunno, 2002: Mesoscale predictability of the "surprise" snowstorm of 24–25 January 2000. *Mon. Wea. Rev.,* **130,** 1617–1632.